Theoretical Modeling of SiO_2 Photochemical Vapor Deposition and Comparison to Experimental Results for Three Oxidant Chemistries: $SiH_4 + O_2$, H_2O/O_2, and H_2O_2

Randa Pfeifer Roland† and Roger W. Anderson*

Department of Chemistry and Biochemistry, University of California, Santa Cruz, California 95064

Received September 5, 2000. Revised Manuscript Received April 25, 2001

An elementary model, independent sheet simulation of photochemical vapor deposition (ISSPCVD), is introduced that illustrates the roles of chemical reactions and transport in photochemical vapor deposition (photo-CVD). A simple model for diffusion and integration of a small number of chemical reaction rate equations allows simulations of SiO_2 photo-CVD to be performed, and this work shows that it is possible to assume that one SiO_xH_y intermediate is the dominant precursor to SiO_2 deposition. Three oxidants for use with SiH_4 are investigated: O_2, H_2O/O_2, and H_2O_2. The simulations allow determination of concentrations of important gas-phase species and estimated deposition rates as functions of time, probability of gas-phase species diffusing to the substrate and effective reaction chain length as functions of height, and deposition rate dependence on purge gas identity and vacuum ultraviolet light intensity. The results reflect our experimental results, including the dependence of deposition rate on experimental parameters and the time evolution of film growth, without adjusting known parameters (e.g., absorption coefficients, rate constants). The simulations provide strong support for the important role of the radical chain reaction $OH + SiH_4 = SiH_3 + H_2O$; $SiH_3 + O_2 = SiH_2O + OH$. The simulations provide insight for the mechanism for SiO_2 deposition by the thermal oxidation of SiH_4 by O_2.

Introduction

Chemical vapor deposition (CVD) is widely used in the manufacture of solid-state devices. A variety of parameters govern film growth, such as the nature and importance of gas-phase and surface reactions, gas flow characteristics, temperature, pressure, and so on. To understand and optimize the deposition process, it is desirable to develop a realistic model describing the overall reaction mechanism that includes estimation of expected deposition rates (r_d's) and their dependence on experimental parameters. Simulation of CVD depositions is a very complex problem because chemical reactions, diffusion, and gas flow of many species must be considered. It is particularly difficult to adequately model and quantify a heterogeneous process which involves a significant amount of chemistry in the homogeneous phase, as is the case in many CVD processes. One such system, which is a cornerstone technique used in a variety of industries, is SiO_2 deposition from gas-phase reactants.

During the past 50 years, a variety of deposition methods and reactant mixtures have been investigated for fabrication of SiO_2 films. Thermal oxidation of silicon in the solid state is the major method for forming gate oxide, and sputtering of quartz is a major method for isolation. Conventionally, SiO_2 CVD has been driven thermally, with one of the most widely exploited techniques relying on the oxidation of silane (SiH_4) by oxygen (O_2). SiH_4–N_2/O_2 mixtures at room temperature appear stable up to a maximum of 0.8% SiH_4;[1] however, increasing the temperature, changing the respective gas concentrations, and/or altering system pressure can initiate SiH_4 oxidation and even lead to explosions.[1,2] By exploiting a suitable window of reaction conditions, adherent SiO_2 films can be formed at reasonable deposition rates at relatively low temperatures. As thermally driven techniques lose favor in industry for certain applications,[3] the importance of reduced temperature techniques such as plasma-enhanced CVD (PECVD) has greatly increased. Photochemical vapor deposition (photo-CVD) represents a logical, low temperature alternative to conventional film preparation methods.[4] Photo-CVD, which harnesses UV/VUV radiation of sufficient energy to break chemical bonds, encompasses elemental as well as dielectric and semiconductor compound films.[5]

Certainly thermal CVD of SiO_2 is very complicated to simulate, and to this date there exist no satisfactory comprehensive theoretical and computational results except for the linear and quadratic models[6,7] for silicon

* Corresponding author. E-mail: anderson@chemistry.ucsc.edu.
† E-mail: pfeifer@chemistry.ucsc.edu.

(1) Strater, K. *RCA Rev.* **1968**, *29*, 618.
(2) Ojeda, F.; et al. *J. Mater. Res.* **1998**, *13*, 2308
(3) SEMATECH. *The International Roadmap for Semiconductors*; 1999 ed.; Semiconductor Industry Association: San Jose, CA, 1999; http://www.itrs.net/1999_SIA_Road map/Home.html. See also: SEMATECH. *The National Technology Roadmap for Semiconductors*; 1997 ed.; Semiconductor Industry Association: San Jose, CA, 1997; http://notes.sematech.org/ntrs/PublNTRS.nsf.
(4) Eden, J. G. *Photochemical Vapor Deposition*; Wiley-Interscience: New York, 1992.
(5) González, P.; et al. *Thin Solid Films* **1992**, *218*, 170.

10.1021/cm0007104 CCC: $20.00 © 2001 American Chemical Society
Published on Web 07/10/2001

oxidation to product thermal oxide. Despite decades of research, controversy still remains regarding the relative important of homo- and heterogeneous reactions, the role of gas-phase transport and diffusion phenomena, etc. Modeling plasma-based chemistry is even more complex because it involves a "chemical soup" of reactants, electrons, intermediate species, radicals, electrons, and excited neutrals. However, for photo-CVD, one might expect that simulation of the deposition rates r_d's would be simpler because there are fewer reactive species and fewer necessary reactions. This is not to imply the problem has become trivial; it still involves complex gas-phase and surface processes, etc.

Here we show for the first time that this simplified nature of photo-CVD can result in excellent simulations of depositions that reflect experimentally obtained results, including the dependence of r_d on experimental parameters and the time evolution of film growth. Known constants (e.g., absorption coefficients, reaction rate constants) are not adjusted to make the simulations fit our experimental data. Three oxidants for use with SiH_4 are investigated: O_2, H_2O/O_2, and H_2O_2 (experimental details and results are presented in our experimental paper[8]). A simple model for diffusion and integration of a small number of chemical reaction rate equations allows good simulation of the H_2O/O_2 and O_2 systems both for deposition rates, r_d's, and profiles. The simulations also give most of the features that we observe for the H_2O_2 system, but only with the addition of a new, unknown reaction in the mechanism. We comment briefly on the relationship between our results and the mechanism for thermal SiH_4 oxidation/SiO_2 deposition.

The experimental method used to photochemically deposit SiO_2 films has been described.[8] Briefly, 172 nm light (~2 W/cm^2) provided by a Xe_2^* excimer lamp located approximately 20 cm above the substrate irradiated reactant gases flowing over the wafer surface. About 50 mm of the 100 mm diameter silicon substrate was directly irradiated; any light reflected into the downstream half of the active deposition region probably extended no more than 10 mm. Reactant residence times prior to, during, and downstream of the exposure to vacuum ultraviolet (VUV) radiation were approximately 10, 21, and 17 ms, respectively. This caused the film thickness to vary over the wafer surface along the direction of the gas flow. However, when desired, reaction conditions could be optimized such that the thickness variation over the entire Si wafer is around 1−2%. Process gases were vertically confined to roughly 1.2 cm above the deposition surface, and reactant and purge gases were added so that nominal plug gas flow velocities (~300 cm/s) across the wafer did not change. Here, results for 22.5 sccm SiH_4 with 200 sccm O_2, 300 sccm O_2, 240 sccm H_2O + 200 sccm O_2, or 360 sccm aqueous H_2O_2 in 3400 sccm N_2 or Ar purge gas are compared with those predicted by the model.

There have been numerous efforts to simulate CVD experiments, and very sophisticated methods have been developed. For example, Kleijn has recently published a report that provides a state-of-the-art example of computation modeling of transport phenomena and chemistry in CVD.[9] However, these simulations involve very complicated computations and many parameters that characterize the chemical reactions and transport. The models are so comprehensive that it is unlikely that experimental values will be available for all of the parameters. In some early simulations most of the parameters are adjusted to fit experimental CVD results.[10] However, in more recent simulations some of the parameters that have been adjusted to increase agreement between simulation and experiment include sticking coefficients,[11] the dependence of adsorption equilibria on fractional surface coverage of vacancies,[12] and individual and/or apparent reaction rate constants.[12] Simulations may also be based on a large number of estimated rate constants (vs known)[11] or use another deposition experiment to specify the rate of a surface deposition reaction.[13] Mechanistic interpretation is sometimes also omitted, with only a loose general explanation of the assumed chemistry provided.[13] These modern simulations typically involve very complicated computations, and it becomes difficult or impossible to sort out the importance of homogeneous reactions, heterogeneous reactions, transport, mixing, etc. Also, the mathematics and theory involved in these beautiful models are frequently really only appreciated by specialists in the simulation field.

Our goal in this paper is to introduce a very simple model, independent sheet simulation of photo-CVD (ISSPCVD), that allows a clear picture of the roles of chemical reactions and transport in photo-CVD. The model uses a small set of chemical reactions and a trivial solution to the diffusion equation. No variable parameters are used, yet the model shows clearly the important chemistry in our depositions, as presented in our experimental paper.[8] We introduce first the model, and then the input parameters, results, and discussion.

Theoretical Model

We model the photochemical deposition process with a realistic set of photoinduced and subsequent reactions and a simple treatment of the transport of the reactive intermediates and products to the substrate surface. Rate equations for the relevant chemical reactions (see Table 1) are numerically integrated with boundary conditions corresponding to experimental conditions.[8] The rate equations are integrated with a fourth-order Runge−Kutta method.[14] This nonstiff differential equation integration routine can be used if the rate equations for the O(^{1}D) reactions are treated by the steady-state approximation. Consequently, O(^{1}D) and its reactions can be completely neglected when the reacting gases are not irradiated. With the concentrations and light in-

(6) Deal, B. E.; Grove, A. S. *J. Appl. Phys.* **1965**, *36*, 3770.
(7) Lewis, E. A.; Irene, E. A. *J. Vac. Sci. Technol., A* **1986**, *4*, 916.
(8) Roland, R. P.; Bolle, M.; Anderson, R. W. *Chem. Mater.* **2001**, *13*, 2493.
(9) Kleijn, C. R. *Thin Solid Films* **2000**, *365*, 294.
(10) Grabiec, P. B.; Przyłuski, J. *Surf. Technol.* **1985**, *25*, 307. Grabiec, P. B.; Przyłuski, J. *Surf. Technol.* **1985**, *25*, 315. Grabiec, P. B.; Przy_uski, J. *Surf. Technol.* **1986**, *27*, 219.
(11) Dollet, A.; et al. *Plasma Sources Sci. Technol.* **1995**, *4*, 94.
(12) Kuijlaars, K. J.; et al. *Mater. Sci. Semicond. Process.* **1998**, *1*, 43.
(13) Wolf, H.; et al. *Microelectron. Eng.* **1999**, *45*, 15.
(14) Teukolsky, S. A.; Vetterling, W. T.; Flannery, B. P. *Numerical Recipes in Fortran,* 2nd ed.; W. H. Press: Cambridge, New York, 1992; p 704.

Table 1. Rate Constants Used for the Simulations

no.	reaction	rate constant[a]	ref[a]
1	$O_2 + h\nu \rightarrow O(^1D) + O(^3P)$	$k_1 = 1.44 \times 10^{-19} I_{172}$[b]	15
2	$H_2O + h\nu \rightarrow H + OH$	$k_2 = 3.72 \times 10^{-18} I_{172}$	15
3	$H_2O_2 + h\nu \rightarrow 2OH$	$k_3 = 3.0 \times 10^{-18} I_{172}$	15
4	$O(^1D) + N_2 \rightarrow O(^3P) + N_2$	$k_4 = 2.4 \times 10^{-11}$	15−18
5	$O(^1D) + Ar \rightarrow O(^3P) + Ar$	$k_5 = 0$	15−18
6	$O(^1D) + H_2O \rightarrow 2OH$	$k_6 = 2.2 \times 10^{-10}$	15, 18
7	$O(^3P) + SiH_4 \rightarrow SiH_3 + OH$[c]	$k_7 = 0.9 \times 10^{-12}$	19
8	$OH + SiH_4 \rightarrow SiH_3 + H_2O$[d]	$k_8 = 1.4 \times 10^{-11}$	19
9	$SiH_3 + O_2 \rightarrow SiH_2O + OH$	$k_9 = 1.3 \times 10^{-11}$	20
10	$H + H_2O_2 \rightarrow H_2O + OH$	$k_{10} = 1.2 \times 1013$	18
11	$H + SiH_4 \rightarrow SiH_3 + H_2$	$k_{11} = 2.1 \times 1013$	20
12	$OH + OH \rightarrow H_2O + O(^3P)$	$k_{12} = 1.8 \times 10^{-12}$	18
13	$SiH_3 + SiH_3 \rightarrow SiH_4 + SiH_2$	$k_{13} = 7.9 \times 10^{-11}$	20
14	$SiH_3 + OH \rightarrow SiH_2O + H_2$[e]	$k_{14} = 1.0 \times 10^{-11}$	
15	$O(^1D) + SiH_4 \rightarrow SiH_2O + H_2$[e]	$k_{15} = 2.2 \times 10^{-10}$	
16	$SiH_3 + H_2O_2 \rightarrow SiH_2O + OH + H_2$[e]	$k_{16} = 1.2 \times 10^{-10}$	

[a] Rate constants for k_1, k_2, and k_3 in s^{-1}, others in cm^3 $molecule^{-1}$ s^{-1}. [b] I_{172} is the VUV intensity in photons cm^{-2} s^{-1}. [c] Reference 19 gives $k_7 \sim (0.48-1.12) \times 10^{-12}$ over 297.0−437.8 K; refs 21−23, $\sim 3.5 \times 10^{-13}$. [d] Reference 19 gives $k_8 \sim (1.24-1.30) \times 10^{-11}$ over 299.6−425.8 K. [e] Estimated.

tensities considered in this paper, an integration step size of 0.5 μs was suitable for our calculations, and the rate equations are integrated for as long as 100 ms. The model does not treat heterogeneous reactions on the substrate surface, but rather simply uses the transport rate of a critical intermediate (SiH_2O) to yield an estimate for the absolute deposition rate, r_d, in angstroms per minute (Å/min). Despite the simplifications, the overall model provides a good simulation of experimental results without resorting to fitting techniques that involve adjusting known constants to better fit the data.

The transport of film precursors (i.e., SiH_2O) to the surface is a complicated process that involves diffusion of species with varying diffusion coefficients in three dimensions, convection, mixing of different gas flows, laminar flow, and boundary layers. This transport must compete with the flow velocity of the gases across the wafer which sweeps most of the film precursors to the chamber exhaust. The net result of the transport and the gas flow velocity is that less than 1% of the film precursors produced in the gas phase will reach the substrate surface. We show that transport processes can be greatly simplified and diffusion in one dimension can be assumed to calculate the r_d's.

Here we present a simple, physically reasonable treatment of this transport that can be calculated in a reasonable period of time and that is based on sensible diffusion coefficients and flow velocities. We neglect convection and mixing, and we assume that only one-dimensional diffusion in the direction perpendicular to the substrate needs to be considered. The model assigns the same diffusion coefficient for all species, and we assume constant velocity plug gas flow which neglects boundary layers and laminar flow velocity distributions. To develop the mathematical basis of our diffusion model, we start with the time-dependent diffusion equation in one dimension:

$$\frac{\partial c(z,t)}{\partial t} = D\frac{\partial^2 c(z,t)}{\partial z^2} \qquad (1)$$

where $c(z,t)$ is a concentration that depends on both position and time. We seek a general solution for this equation with the requirement that the concentration is zero at the substrate ($z = 0$). The diffusion equation can be easily solved by separation of variables, and the following sine series expression satisfies the boundary condition at $z = 0$.

$$c_h(z,t) = \sum_{n=1}^{n_{max}} a_n \exp(-Dk_n^{\ 2}t)\sin(k_n z) \qquad (2)$$

where $k_n = n\pi/l$, n is a positive integer, and l is the length of a one-dimensional box extending upward from the substrate. We assume a large value for l so that there is effectively loss of gas phase molecules only for $z = 0$ (substrate surface). The values of a_n depend on $c(z,0)$, and in our case we assume that $c(z,0) = 1/w$ for $h - w \le z \le h$, and 0 otherwise. The $1/w$ ensures that the integral of $c(z,0)$ over z is 1. Hence we assume diffusion from a sheet of gas of thickness, w, that is moving across the substrate with its bottom at a distance $h - w$ above the substrate. For this choice we obtain the following expression for a_n:

$$a_n = \frac{2}{l}[\cos(k_n(h - w) - \cos(k_n h))]/(k_n w) \qquad (3)$$

It is also consistent with this model to assume that the initial concentration profile in a slab is a δ function centered at $z = h$; then

$$a_n = \frac{2}{l}\sin(k_n h) \qquad (4)$$

Now the probability for diffusion of molecules from the sheet to the substrate is given in terms of $P_h(t)$, which is the probability of remaining in the gas phase at time, t, from a sheet at distance h above the substrate. The series is cumbersome for early time steps

$$P_h(t) = \int_0^l c_h(z',t)\,dz' = \sum_{n=odd}^{n_{max}} 2a_n \exp(-Dk_n^{\ 2}t)/(k_n l) \qquad (5)$$

where as many as 10000 terms may be required. However, many fewer are required for longer times because the exponential in t becomes negligible for large values of n.

We now complete the specification of our model. The rate equations in Table 1 are integrated for many time steps, and at the end of each interval the concentrations of the radical species and the deposition precursor are adjusted for diffusion. For example, the loss of SiH_2O to the substrate is in the interval from $t - \Delta t$ to t is given by

$$\delta_{SiH_2O}(t,h) = (P_h(t-\Delta t) - P_h(t))n_{SiH_2O}(t) \qquad (6)$$

where the last term is the concentration of SiH_2O at time t. This equation assumes that SiH_2O is deposited with a sticking coefficient equal to 1. Similar expressions are used for O and H atoms, OH, and SiH_3, with the calculations performed for sticking coefficients between 0 and 1. We assume that a SiO_2 unit is deposited whenever a SiH_2O or SiH_3 molecule strikes and sticks to the substrate. Also, the concentration of the stable gases O_2, H_2O, H_2O_2, and SiH_4 do not decrease because

of diffusion to the substrate, but O_2 and H_2O_2 concentrations are decreased to fully oxidize SiH_2O that strikes the substrate.

Our model also yields an estimate for the absolute r_d in Å/min. The number of SiO_2 units per cm^3 of solid, n_{SiO_2}; the time increment, Δt; and the flow velocity, v, in cm/s can be combined to give the deposition rate, $r_d(t)$, as

$$r_d(t) = \frac{60 \times 10^8 w}{\Delta t n_{SiO_2} v} \int_0^{h_{max}} \delta_{SiH_2O}(t,h)\, dh \qquad (7)$$

The average deposition rate, $\bar{r}_d$, over the measured part of the substrate is given as

$$\bar{r}_d = \frac{1}{t_d - t_u} \int_{t_u}^{t_d} r_d(\tau)\, d\tau \qquad (8)$$

where the upstream and downstream times, t_u and t_d, are given as $t_u = (x_u - x_e)/v$ and $t_d = (x_d - x_u)/v$. Here x_l is the position where irradiation starts and x_u and x_d are the upstream and downstream positions on the substrate between which the average deposition rate is measured.

The conversion fraction (number of SiO_2 per unit time deposited over a substrate region bounded by the width of the substrate region, w_s, and x_u and x_d divided by the number of SiH_4 molecules flowing over the substrate per unit time) is also easily calculated:

$$c_f = \frac{w_s(x_d - x_u)\bar{r}_d n_{SiO_2} \times 10^{-8} \times 22414}{Q_{SiH_4} N_{Av}} \qquad (9)$$

In summary, this reaction/diffusion model calculates the reaction and rates as if the reactant and intermediate concentrations in the sheet are determined by the rate equations and $P_h(t)$. However, it is clear that diffusion spreads the initial sheet concentration profile. The main reason that the model appears to work is that the diffusion from one sheet to others is to a large degree compensated by diffusion from other sheets. Another implicit assumption is that the diffusion from the sheets at the largest distance from the substrate does not significantly increase the height of the reacting gases. Also, this simple treatment of rates should be most realistic for reactions with reactant gases and less valid for radical−radical recombination.

Input Data

We use the reactions in Table 1 to describe the chemistry for photo-CVD of silicon dioxide at 172 nm. All of the rate constants (given in cm^3 molecule^{-1} s^{-1}) are literature values, except we use estimated rate constants for reactions 14−16. We use constants that correspond roughly to kinetic cross sections for reactions 15 and 16. A smaller rate constant is used for the radical−radical reaction 14, because the products for this reaction probably result from a long-lived complex that must compete with the abstraction reaction that produces $SiH_2 + H_2O$. However, as we will see later, the deposition results are quite insensitive to the value for k_{14}. The rates of the photolysis reactions 1−3 depend on the photolysis light intensity in photons cm^{-2} s^{-1} and on the concentration in molecules cm^{-3} of the reactant gases O_2, H_2O, and H_2O_2. The photolysis reactions only occur where there is irradiation of the reactant gases. The other reactions in Table 1 produce and destroy reactive intermediates and produce the deposition precursor, SiH_2O. We have set the rate constant, k_5, to zero for the quenching of O(^{1}D) by argon. The rate constant for reaction 7 is a matter of some debate. Room temperature values range from roughly 0.35×10^{-12} to 1.2×10^{-12}; at 100 °C (373 K) k_7 should be somewhere on the order of 0.9×10^{-12}.[18,21−23] The inclusion of the SiH_3/H_2O_2 reaction (no. 16), although somewhat unprecedented, appears necessary in the H_2O_2 simulation. Its rate has not been established, but based on the reactivities of the species involved, it is reasonable to suggest that it proceeds close to or at the gas kinetic limit. Under the operating conditions for photo-CVD, we may consider all the reactions in Table 1 to be irreversible. The recombination of the products of the photolysis reactions will be slow because of the low concentration of the radical species, and by the likely necessity of a third body. The other reactions in Table 1 are exoergic by at least 100 kJ mol^{-1}, so the reverse reactions are endoergic and hence will have small rate constants.

Our results also show that it is possible to assume that one SiO_xH_y intermediate (i.e., SiH_2O) is the dominant precursor leading to SiO_2 deposition, so that its production and transport determine the rate of film growth. As indicated in Table 1, SiH_2O can be generated by four processes. Little is known about reactions 14−16. Reaction 9, a key step in the O_2 and H_2O/O_2 systems, probably proceeds through the activated complex, SiH_3O_2*, which may decompose according to [2,18,22]

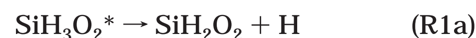

$$SiH_3O_2^* \rightarrow SiH_2O_2 + H \qquad (R1a)$$

$$\rightarrow SiH_2O + OH \qquad (R1b)$$

$$\rightarrow H_3SiO + O \qquad (R1c)$$

Although each of these SiH_xO_y species represents a possible precursor to film deposition, it is unclear which channel is dominant. Takahashi et al. indicate that reaction R1c experiences a barrier to reaction of roughly 59 kJ/mol, making it unlikely.[24] Reactions R1a and R1b show no potential barrier and a ratio of rate constants, k_{R1a}/k_{R1b}, of approximately 0.26, which suggests that reaction R1b should occur at least 3 times for every reaction R1a.[24] According to calculations performed by Darling and Schlegel using ab initio theory to study the potential energy surface for the SiH_3/O_2 reaction, reaction R1b likely proceeds through a facile process involving unimolecular rearrangement to H_2SiOOH* and subsequent OH elimination.[25] Despite the fact that

(15) Okabe, H. *Photochemistry of Small Molecules*; Wiley-Interscience: New York: 1978.
(16) Snelling, D. B.; et al. *J. Chem. Phys.* **1996**, *44*, 4137.
(17) Katakis, D.; Taube, H. *J. Chem. Phys.* **1962**, *36*, 416.
(18) Atkinson, R.; et al. *J. Chem. Ref. Data* **1997**, *26*, 521. Atkinson, R.; et al. *J. Chem. Ref. Data* **1992**, *21*, 1125.
(19) Aktinson, R.; Pitts, J. N., Jr. *Int. J. Chem. Kinet.* **1978**, *10*, 1151.
(20) Jasinski, J. M.; et al. *Chem. Rev.* **1995**, *95*, 1203.
(21) Agrawalla, B. S.; Setser, D. W. *J. Chem. Phys.* **1987**, *86*, 5421.
(22) Koshi, M.; et al. *J. Phys. Chem.* **1993**, *97*, 4473.
(23) Horie, O.; et al. *J. Phys. Chem.* **1991**, *95*, 4349.
(24) Takahashi, T.; et al. *J. Electrochem. Soc.* **1996**, *143*, 1355. Takahashi, T.; et al. *J. Electrochem. Soc.* **1998**, *145*, 1070.

Table 2. Input Data for Simulations

parameter			relevant
symbol	name	value	eqs
D_0	diffusion coefficient at STP	0.2 cm^2/s	10
α	temperature dependence of D	1.0	10
l	interval for Fourier series	20 cm	2−5
w	width of sheet	0.01 cm	3
h_{max}	height of reacting gas	1.2 cm	7
Δt	integration time step	0.5 μs	
v	gas flow velocity	300 cm/s	7, 8
x_l	position where irradiation begins	−6.3 cm	8
x_u	upstream position on substrate	−4.2 cm	8, 9
x_d	downstream position on substrate	4.2 cm	8, 9
w_s	width of substrate region	26.7 cm	9
n_{SiO_2}	number density of SiO_2	2.31×10^{22} SiO_2/cm^3	7, 9
P	total pressure	7 mmHg	
T	gas temperature	373 K	

inclusion of reaction R1c was required to explain the measured H_2/H_2O ratio in SiH_4/O_2 explosions, RRKM calculations with empirical estimation of transition state properties also favor reaction R1b.[26] Koshi et al. have measured the branching ratio for reactions R1a, R1b, and R1c to be 0.65, 0.25, and 0.10, respectively; however, certain aspects of their results seem questionable. For example, first-order decay processes caused by diffusion of H and SiH_3 to the walls were included, but similar losses for OH were ignored.[22] The extremely fast reaction of OH with SiH_4 may also occur to a greater degree than the researchers predict, causing the measured OH concentration to appear lower than it initially is via reaction R1b (vs the H/SiH_4 reaction for H atom loss, which is very slow and unlikely to contribute to H atom loss). Darling and Schlegel, who were unable to identify an energetically feasible unimolecular process leading to H production, have suggested that H atoms might instead result from the reaction[25]

$$SiH_2O + OH \rightarrow HSi(O)OH + H \qquad (R2)$$

which has a rate constant on the order of 1.7×10^{-11}.[24] Koshi et al. do not include reaction R2 in their overall mechanism.[22] Therefore, it seems reasonable to treat SiH_2O as the dominant SiO_xH_y intermediate in SiO_2 formation. The results presented below support this assumption.

Other parameters used in the simulations are presented in Table 2. The diffusion coefficient, D, is assumed to depend on T and p according to

$$D = D_0\left(\frac{T}{T_0}\right)^{\alpha}\left(\frac{p_0}{p}\right) \qquad (10)$$

In this work α is assumed to be 1.0. Often α is given a value of 1.75, which yields a value of D that is 26% larger at $T = 373$ K than the value used in this work. The sensitivity analysis in Table 4 shows that using a larger diffusion coefficient will not significantly affect the results. The values of h_{max}, v, x_l, x_u, x_d, w_s, P, and T reflect the experimental values.[8] The values of l, w, and Δt are chosen to provide converged results for the simulations.

(25) Darling, C. L.; Schlegel, H. B. *J. Chem. Phys.* **1994**, *98*, 8910.
(26) Hartman, J. R.; et al.. *Combust. Flame* **1987**, *68*, 43.

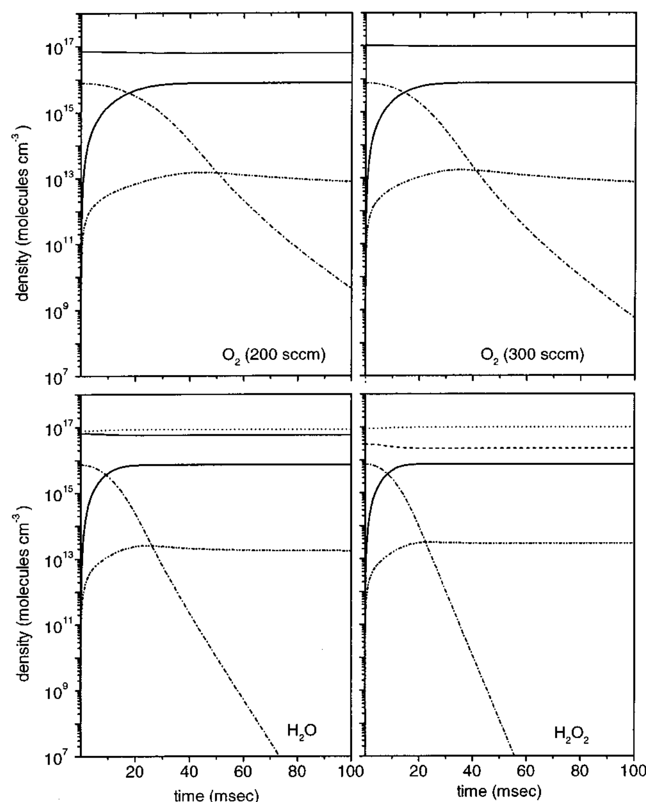

Figure 1. Time profiles for the reactants, products, and major intermediates for each of the oxidant chemistries (− · −, SiH_4; −, O_2; ···, H_2O; H_2O_2; − ·· −, OH; bold −, SiH_2O).

Results

Time profiles for the reactants, products, and major intermediates when there are no losses due to heterogeneous reactions are shown in Figure 1. These time profiles are obtained by integration of the kinetic rate equations without any diffusive loss of products. The boundary conditions correspond to the experiments.[8] Two plots are shown for O_2, corresponding to two flow rates (200 and 300 sccm, respectively). Some key findings are worth emphasizing. The SiH_4 concentration is depleted to different extents in the presence of the various oxidants. With O_2, the amount of SiH_4 has dropped by a factor of roughly 1000 by the time the reactants reach the back edge of the wafer; for H_2O and H_2O_2, SiH_4 depletion is essentially complete. In the O_2 system, the SiH_2O trace is coincident with that of H_2O except at the very shortest times, which is consistent with a net stoichiometry of $SiH_4 + 2O \rightarrow SiH_2O + H_2O$. It also appears that self-recombination of OH radicals may be a significant channel of OH loss.

Figure 2 depicts the ratio of the rate of SiH_2O production to the rate of primary photoproduct production as a function of time for each system. This ratio represents the "effective chain length" as function of time. The chain length can be as large as 1700! The reaction chemistry initiated with H_2O and H_2O_2 photolysis appears to be extremely efficient in depleting SiH_4 and, consequently, in producing SiH_2O. The OH generated at early times in the H_2O and H_2O_2 system clearly leads to rapid SiH_4 consumption through a self-perpetuating chain with the reactions $OH + SiH_4 = SiH_3 + H_2O$ and $SiH_3 + O_2 = SiH_2O + OH$. With the O_2 chemistry, the peak shifts to later time. Because O_2

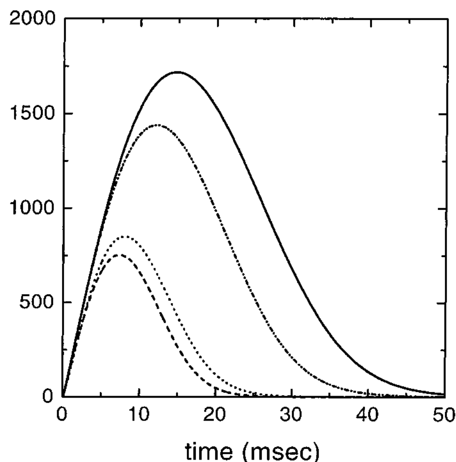

Figure 2. Ratio of the rate of production of SiH_2O to the rate of production of primary photoproducts as a function of time (—, 200 sccm O_2; — ·· —, 300 sccm O_2; ···, 240 sccm H_2O + 200 sccm O_2; - - -, 360 sccm H_2O_2).

has a σ_{172} value approximately 4–5 times lower that that of H_2O and H_2O_2,[15] primary photolysis produces fewer reactive species, and O atoms are less effective at initiating the steps leading to deposition intermediates. It should be kept in mind that the SiH_4/O reaction rate constant is at least an order of magnitude smaller than that for SiH_4/OH. Strictly speaking, the plots are valid up to $t = 21$ ms (i.e., $x = 0$ mm), the time (position) at which the light is effectively turned off. The curves for times after 21 ms show the deposition rate (SiH_2O production) normalized by the photolysis product rate that would have been produced had the light been on. For the H_2O_2 and H_2O chemistries, the ratio has essentially dropped to zero by this time; for O_2, the ratio has peaked and begun to drop by $t = 21$ ms; past this point, the chain is still operative despite the fact that no new photoproducts are being generated.

In Figure 3a (upper plot), the fraction, $1 - P_h(t)$, of species diffusing to the surface from different heights above the substrate as a function of time, which translates into position along the wafer surface, is shown. Clearly, those species that are close to the wafer have a great possibility of reaching the surface in a short time, while the fraction drops rapidly as height increases. For example, more than 90% of molecules in sheets with h less than 0.2 cm diffuse to the substrate within 50 ms, while less than 50% encounter the substrate for h greater than 1.2 cm. This also points out how important gas flow characteristics can be in determining the characteristics and rate of deposition. Perhaps an even more interesting finding is that much deposition results from species at relatively large distances from the wafer surface. At first this may seem counterintuitive, if it is assumed that deposition results mainly from the species that are close to the wafer (i.e., having the greatest probability of diffusing to the surface). However, if one looks at the "effective chain length" for the H_2O/O_2 chemistry at different heights above the wafer over the deposition surface (Figure 3b, lower plot), it becomes clear that the chain length of the gas-phase reactions is critical. Very close to the wafer, reactive species rapidly diffuse to the surface, and there is little time for the photochemically initiated chain reactions to progress. The effective chain length becomes

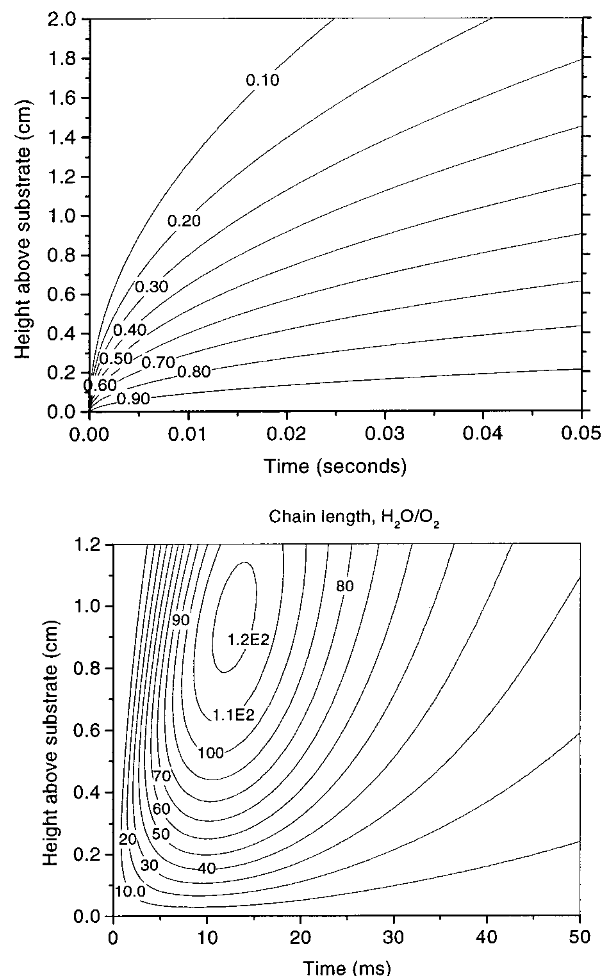

Figure 3. (a, upper) Fraction of species diffusing to the surface from different heights above the substrate as a function of time (and hence position along the wafer surface). The labels on the contours give the fraction. (b, lower) Ratio of the net rate of production of SiH_2O to the rate of production of primary photoproducts at different heights above the wafer as a function of time.

greater at greater distances because gas-phase intermediates have more time to react before they reach the deposition surface.

Table 3 summarizes some of the results available from our simulations. The table contains calculated and observed average deposition rates, $\bar{r}_d$, their ratio (given as a percent, (calculated/experimental) × 100%); and the conversion fraction (eq 9). A cursory comparison of the calculated and observed average deposition rates might suggest poor agreement. However, our simulations do not include all of the important parameters that contribute to the deposition processes, such as mixing, convection, flow velocity distribution, laminar flow, and intermixing between layers. The fact that we calculate values that are within an average factor of 3 of the experimental data is quite remarkable. Based on the conversion data, it is also clear that a very small fraction of the input reactant gases actually contributes to deposition on the wafer surface.

Figure 4 shows comparisons of the experimental (solid line) and model (dotted line) data for each system. The x-axes correspond to the distance along the wafer; the left and right y-axes correspond to the experimental and simulated r_d's, respectively. While there are some dis-

Table 3. Calculated and Experimental Deposition Rates and the Overall Conversion of Reactants to Deposition for a Variety of Reactant Flow Rates for Each Oxidant System

oxidant flow (sccm)[a]	deposition (Å/min)		calcd/ exptl (%)	conversion ($R \rightarrow D$)[b]
	calcd	exptl		
120 H_2O				
100 O_2	38	110	34	3.22×10^{-3}
200 O_2	42	137	31	3.61×10^{-3}
300 O_2	44	143	31	3.76×10^{-3}
240 H_2O				
100 O_2	45	143	31	3.81×10^{-3}
200 O_2	47	187	25	4.00×10^{-3}
11.3 SiH_4	24	125	19	4.01×10^{-3}
300 O_2	48	211	23	4.04×10^{-3}
360 H_2O				
100 O_2	48	169	28	4.05×10^{-3}
200 O_2	49	239	20	4.15×10^{-3}
300 O_2	49	259	19	4.14×10^{-3}
120 H_2O_2	36	75	48	3.08×10^{-3}
240 H_2O_2	47	156	30	4.02×10^{-3}
11.3 SiH_4	24	120	20	4.06×10^{-3}
360 H_2O_2	51	225	23	4.33×10^{-3}
11.3 SiH_4	26	194	13	4.35×10^{-3}
200 O_2	29	35	83	2.45×10^{-3}
300 O_2	36	53	67	3.01×10^{-3}
11.3 SiH_4	18	35	52	3.03×10^{-3}
400 O_2	39	134	29	3.32×10^{-3}

[a] At 22.5 sccm SiH_4 unless otherwise indicated. [b] Fraction of the limiting reactant that appears as deposition (SiH_2O) on the substrate area.

crepancies in r_d's, the agreement between the time evolution of the deposition is very good, with slight differences apparent between the chemistries. The simulated data tends to peak a bit late in the O_2 system but early in the H_2O/O_2 case. This may be partially explained by the fact that one diffusion coefficient was assumed for all species present, as well as the factors related to gas flow that were neglected (see above). The model was not able to reproduce the experimentally observed profile for the H_2O_2, suggesting that additional unknown steps are probably involved in the deposition chemistry.

$O(^1D)$, one possible product of O_2 photolysis at 172 nm, has been suggested to play a key role in photo-CVD experiments.[5] $O(^1D)$ is rapidly deactivated by N_2, while Ar is essentially inert, so profound differences in deposition might be expected by switching the purge gas from N_2 to Ar, particularly in the O_2 system. Figure 5 shows the simulated deposition for experiments conducted with N_2 and Ar. These curves are generated assuming that $O(^1D)$ only reacts via an insertion reaction with SiH_4 according to the expression $SiH_4 + O(^1D) \rightarrow SiH_2O + H_2$, whereas $O(^3P)$ only undergoes an abstraction reaction. The simulation shows that there is no significant difference for the H_2O/O_2 and H_2O_2 systems when the purge is changed from N_2 to Ar, while deposition drops significantly and peaks further downstream in the O_2 system. Experimentally,[8] $\bar{r}_d$ and $r_d(t)$ in the H_2O/O_2 system changed by less than 2% when the purge was changed from N_2 to Ar. For the O_2 system $\bar{r}_d$ decreased by 7% when Ar was used as the purge instead of N_2. The difference between the simulations and the experimental results might be evidence for a number of factors: $O(^1D)$ may not be produced as 50% of the O_2 photodissociation, $O(^1D)$ may experience some gas-phase collisional deactivation in Ar collisions, and/or some or much of $O(^1D)$ may abstract H atoms from SiH_4 rather than inserting into a SiH bond. Again it is clear that most deposition is produced by chain reactions and not by reactions of primary photolysis products.

Another result is the $\bar{r}_d$ as a function of the intensity of the VUV light that provides the photolysis. Figure 6 shows the dependence of the $\bar{r}_d$ for each oxidant system as a function of VUV intensity (in mW/cm^2). Each curve increases and then levels out at as the light becomes more intense. H_2O_2 increases the most rapidly, followed by H_2O and O_2 (with the higher flow rate faster than the lower). The former two are effectively "saturated" at lower light intensities, as might be expected based on their relatively high σ_{172} values. In our experimental work, we have found that r_d appears to increase linearly with VUV power, which appears to be valid for light intensities less than 2 mW cm^{-2} based on the plots shown in Figure 6. The $\bar{r}_d$'s should not scale linearly at higher intensities.

Table 4 provides some sensitivity analysis for $\bar{r}_d$. In particular, it shows the effect of changing the rate constant for the reaction between OH and SiH_3, changing the size of the diffusion coefficient, the 172 nm light intensity, the flow velocity, and the sticking coefficient for O, H, SiH_3, and OH. I_{VUV} and the flow velocity, v, have a large effect on the deposition rates, while changing the rate constant for reaction 14 (Table 1) and using the δ function concentration profile (eq 4) have very little effect.

We have used this simulation model to study the temperature dependence for $\bar{r}_d$. The temperature-dependent rate constants determined from the E_a and preexponential terms (A factors) in Table 5 are used in these simulations. If the number density and hence flow velocity is kept constant for temperatures between 100 and 200 °C, the simulations show small activation energies of 0.3 kJ/mol for the O_2 system and 0.17 kJ/mol for the H_2O/O_2 system. These E_a values are substantially smaller than those that we report in our experimental paper.[8] If the number density is scaled as T^{-1}, the simulations exhibit $\bar{r}_d$'s that decrease with temperature! A lower number density implies fewer photodissociations and secondary reactions as well as a faster velocity that decreases deposition because it is proportional to v^{-1}. Since most of the gas flowing in our experiments is purge gas that is added above the ~1 cm layer of reacting gases, it is likely that the mean temperature of the entire flowing gas does not change much as the substrate temperature is varied.

Discussion

Our work clearly shows the importance of sustained linear chains proceeding in the gas phase for photo-CVD. Primary photolysis reactions provide direct generation of reactive oxidant radicals that can initiate and/or propagate chain reactions. Surface phenomena are also undoubtedly important; however, there is no question that homogeneous processes are very important in determining the deposition rate.

Our simple model provides satisfactory estimates for the deposition rates and good simulations for the time evolution of the deposition. However, the observed average deposition rates are about 3 times larger than those predicted by the simulations. The sensitivity analysis shows that changes in the flow velocity or the

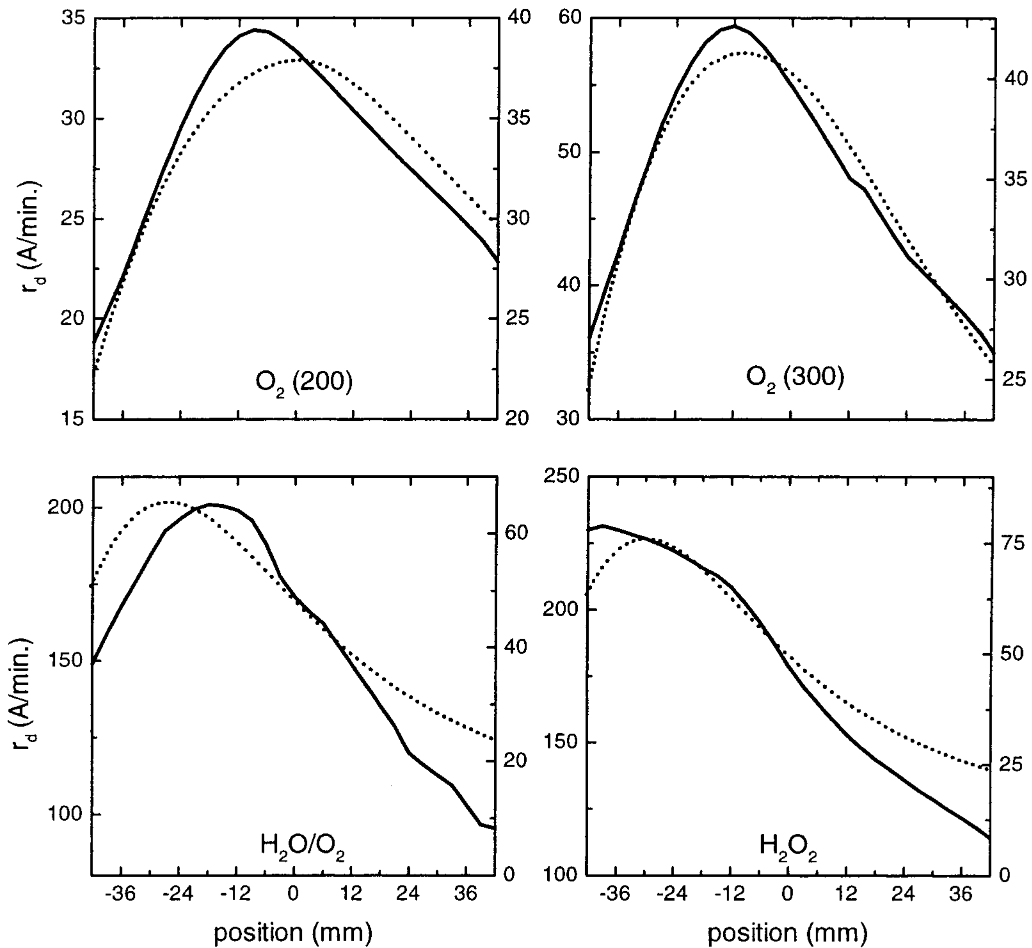

Figure 4. Time evolution of the experimental (—) and model (···) data for each oxidant system. The left scale corresponds to the experimental data, and the right scale is for the model data.

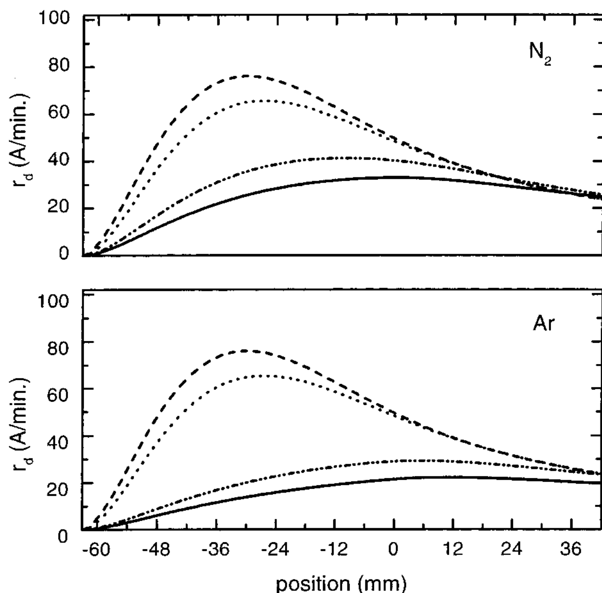

Figure 5. Simulated deposition profiles for experiments conducted in N_2 or Ar purge gas (—, 200 sccm O_2; — ·· —, 300 sccm O_2; ···, 240 sccm H_2O + 200 sccm O_2; - - -, 360 sccm H_2O_2).

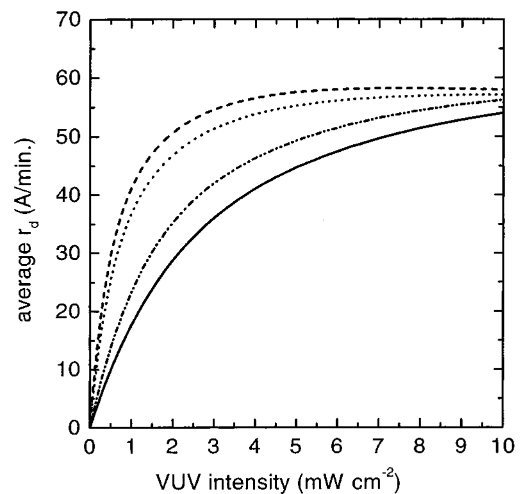

Figure 6. Average deposition rate dependence on total VUV light intensity (mW/cm^2) (—, 200 sccm O_2; — ·· —, 300 sccm O_2; ···, 240 sccm H_2O + 200 sccm O_2; - - -, 360 sccm H_2O_2).

VUV intensity cause large changes in the deposition rate. Consequently, the assumption of constant velocity plug flow may be an important reason for the underestimation of the deposition rate. The velocity distribution for laminar flow would tend to increase the deposition rate because the gases would be moving slower than plug flow near the wafer. Our estimate of the experimental VUV intensity might also be too small, which would also underestimate the deposition rate. However, if the VUV intensity were much larger, r_d would tend to have its maximum value further upstream on the wafer. Convection, the cross-flows of reactive and purge gases, and incomplete mixing might also have large effects, but our simple model provides no information about the effects of these important processes on the

Table 4. Sensitivity Analysis Percentage Change (%) in the Average Deposition Rates for Changes in the Model Input Parameters[a]

	300 sccm O_2	200 sccm O_2	240/200 sccm H_2O/O_2	360 sccm H_2O_2
$(1/2)k_{14}$[b]	0.6	0.9	0.5	0.1
$2k_{14}$[b]	−1.1	−1.8	−1.1	−0.3
$(1/2)D$[c]	9.7	10.8	7.2	6.6
$2D$[c]	−17.5	−18.0	−16.1	−15.8
$(1/2)I_{VUV}$[d]	−33.8	−38.7	−21.4	−18.7
$2I_{VUV}$[d]	31.4	42.9	14.9	11.6
(1/2)velocity[e]	163.2	202.8	107.5	95.8
2 velocity[e]	−56.8	−61.8	−41.2	−36.2
sticking coeff[f] = 0	6.7	8.4	3.4	2.9
δ function[g]	0.6	0.6	0.6	0.6

[a] The changes are referred to the nominal conditions for the results in Table 2. A positive change indicates that the average deposition rate increases with the new condition. In the sensitivity analysis only one parameter is changed at a time. [b] k_{14} is the Table 1 rate constant for $SiH_3 + OH \rightarrow SiH_2O + H_2$. [c] D is the diffusion constant assumed to be 0.2 cm^2/s at STP. [d] VUV intensity is 2.0 mW cm^{-1} for the nominal conditions. [e] The gas flow velocity across the substrate is 300 cm/s for the nominal conditions. [f] This calculation assumes that the sticking coefficients for SiH_3, OH, O, and H are zero. [g] This calculation is done for nominal conditions but with Fourier coefficients given by eq 4.

Table 5. Estimated Activation Energies and Preexponential Terms for Selected Reactions[a]

reaction	E_a	A	ref
$SiH_4 + OH \rightarrow SiH_3 + H_2O$	0.4	1.44×10^{-11}	19
$SiH_4 + O \rightarrow SiH_3 + OH$	6.6	6.84×10^{-12}	19
$SiH_4 + H \rightarrow SiH_3 + H_2$	10.5	1.73×10^{-10}	38
$SiH_4 \rightarrow SiH_2 + H_2$	251	6.17×10^{15}	39
$SiH_4 \rightarrow SiH_3 + H$	390	3.69×10^{15}	38

[a] Values are the best estimates for use in the expression $A \exp(-E_a/RT)$. E_a's are in kJ/mol; A factors for the first three reactions have the units cm^3 molecule^{-1} s^{-1}, and for the unimolecular reactions the unit s^{-1}.

deposition rate. However, most of the neglected processes should have similar effects for the three different chemistries, so although the model underestimates the deposition rates by about the same factor, the deposition profiles are well represented.

Column 4 in Table 3 shows that the ratio of calculated to experimental deposition rates tends to decrease with increasing oxidant concentration. The calculated rates do not increase as quickly with oxidant concentration. This effect is most pronounced for the O_2 chemistry, and this might show that one or more important reaction is missing in the model. Also, this trend may indicate that the important film precursor is not simply SiH_2O but rather a more oxidized silicon species. Surface oxidation reactions may also need to be invoked to explain this tend.

Despite a large amount of kinetic data that is available on the SiH_4/O_2 system, the mechanism of thermal SiH_4 oxidation/SiO_2 deposition is still a matter of debate. Experimentally, SiO_2 deposition rates have been found to depend on a number of experimental parameters, such as temperature, pressure, total gas flow rate, concentration of SiH_4, and O_2:SiH_4 ratios, as well as reactor configuration/size and changes in gas stream flow patterns.[1,2,27,28] The threshold temperature for deposition also appears to depend heavily on these parameters, with values typically lying between 200 and 500 °C; however, deposition has been found at temperatures as low as 140−150 °C.[1,28,29]

It has been suggested that deposition occurs via heterogeneous reactions between SiH_4 and O_2 on the surface of the heated substrate, with gas-phase homogeneous reactions largely ignored.[2,3,27,30−33] A second more plausible reaction mechanism that is supported by our work postulates that SiH_4 oxidation proceeds through a branching chain process characterized by abundant formation of highly reactive free radicals in the gas phase.[1,2,34,35] The reaction of SiH_3 with O_2 molecules plays a key role by making available partially oxidized silicon species in conjunction with chain-carrying radicals, and SiO_xH_y's are very reactive precursors to SiO_2; OH, O, and H propagate the chain and generate new SiH_3 radicals.[2,24,25,34−37] Clearly, as our work shows, once radical species are generated, it is reasonable to hypothesize that reactions proceeding in the gas phase will dominate SiH_4 oxidation.

Extracting an accurate apparent E_a for the overall SiH_4 oxidation/SiO_2 deposition process is complex. The impact of a reaction's E_a and preexponential (A) factor hinges upon residence time and gas flow characteristics in the reactors, which might explain the wide range of E_a's reported for the overall process (2.8 kJ/mol [27] and as high as 33.5 kJ/mol,[1] even at comparable temperatures). Our work does indicate that there must be a low E_a path to produce chain initiators (i.e., H, O, OH, SiH_2, or SiH_3), and we have found SiO_2 photo-CVD to proceed with little or no E_a (roughly 9, 7.5, and 5 kJ/mol for the O_2, H_2O_2, and H_2O/O_2 chemistries).[8] It is clear that the presence of VUV radiation can result in an exceptional reduction in the E_a observed for the deposition process.

Conclusions

In general, it is very difficult to adequately model CVD systems, but this task becomes even more complex when deposition is the result of both homo- and heterogeneous reactions. Relative to thermal and plasma deposition conditions, it might be expected that photo-CVD might be simpler to simulate because fewer species are involved. Here, we develop a reasonable simple model based on a minimal number of rate equations and the integration of differential equations for the gas-phase species. It is possible to obtain good simulations that reflect the dependence of deposition rates on experimental parameters as well as the overall time evolution of the deposition on the wafer surface, even with the assumption that only one SiO_xH_y is the primary intermediate precursor to SiO_2 deposition. Good agreement is obtained between calculated and experimental

(27) Baliga, B. J.; Ghandhi, S. K. *J. Appl. Phys.* **1973**, *44*, 990.
(28) Bennett, B. R.; et al. *Appl. Phys. Lett.* **1987**, *50*, 197.
(29) Results from this laboratory.
(30) Bennett, B. R.; et al. *J. Electrochem. Soc.* **1987**, *134*, 2517.
(31) Cobianu, C.; Pavelescu, C. *J. Electrochem. Soc.* **1983**, *130*, 1888.
(32) Pavelescu, C.; Cobianu, C. *J. Mater. Sci. Lett.* **1988**, *7*, 1988.
(33) Laidler, K. J. *Chemical Kinetics*; Harper and Row: New York: 1987; pp 241−273.
(34) Vasiliev, L. L.; et al. *Thin Solid Films* **1978**, *55*, 221.
(35) Vasiliev, V. V.; et al. *Thin Solid Films* **1981**, *76*, 61.
(36) Koda, S.; Fujiwara, O. *Twenty-first Symposium (International) on Combusion*; The Combustion Institute: Pittsburgh, PA, 1986.
(37) Kondo, S.; et al. *Combust. Flame* **1995**, *101*, 170.
(38) Coltrin, M. E.; et al. *J. Electrochem. Soc.* **1984**, *131*, 425.
(39) Moffat, H. K.; Jensen, K. F.; Carr, R. W. *J. Phys. Chem.* **1991**, *95*, 145.

results for three SiH_4 oxidant systems, O_2, H_2O/O_2, and H_2O_2, and our work clearly demonstrates the importance of chain reactions in these systems. Calculated deposition rates are approximately 3−4 times lower than those obtained experimentally, but this is still rather remarkable in light of the simplicity of the model and the parameters that were neglected or unknown (particularly those related to gas flow; e.g., mixing, convention, velocity distributions, laminar vs plug flow). It is also important to note that known constants (e.g., absorption coefficients, reaction rate constants) were not adjusted to force the simulation to fit the experimental data. Our demonstration of the importance of sustained gas-phase linear chain reactions in the overall deposition process should also be important in thermal and even plasma-assisted SiH_4 oxidation. Photo-CVD also allows significant reduction in the overall activation energy for the deposition process, relative to thermally driven SiO_2 film formation.

CM0007104